View metadata, citation and similar papers at core.ac.uk

brought to you by CORE

provided by Elsevier - Publisher Connector

Neuroscience 169 (2010) 974–986

TWO DISTINCT POOLS OF LARGE-CONDUCTANCE CALCIUM-ACTIVATED POTASSIUM CHANNELS IN THE SOMATIC PLASMA MEMBRANE OF CENTRAL PRINCIPAL NEURONS

W. A. KAUFMANN,[a]* Y. KASUGAI,[a] F. FERRAGUTI[a] AND J. F. STORM[b]

[a]*Department of Pharmacology, Innsbruck Medical University, Peter-Mayr Strasse 1a, 6020 Innsbruck, Austria*

[b]*Centre of Molecular Biology and Neuroscience (CMBN) and Department of Physiology, Institute of Basal Medicine, University of Oslo, PB 1103 Blindern, 0317 Oslo, Norway*

Abstract—Although nerve cell membranes are often assumed to be uniform with respect to electrical properties, there is increasing evidence for compartmentalization into subdomains with heterogeneous impacts on the overall cell function. Such microdomains are characterized by specific sets of proteins determining their functional properties. Recently, clustering of large-conductance calcium-activated potassium (BK_{Ca}) channels was shown at sites of subsurface membrane cisterns in cerebellar Purkinje cells (PC), where they likely participate in building a subcellular signaling unit, the 'PLasmERosome'. By applying SDS-digested freeze-fracture replica labeling (SDS-FRL) and postembedding immunogold electron microscopy, we have now studied the spatial organization of somatic BK_{Ca} channels in neocortical layer 5 pyramidal neurons, principal neurons of the central and basolateral amygdaloid nuclei, hippocampal pyramidal neurons and dentate gyrus (DG) granule cells to establish whether there is a common organizational principle in the distribution of BK_{Ca} channels in central principal neurons. In all cell types analyzed, somatic BK_{Ca} channels were found to be non-homogenously distributed in the plasma membrane, forming two pools of channels with one pool consisting of clustered channels and the other of scattered channels in the extrasynaptic membrane. Quantitative analysis by means of SDS-FRL revealed that about two-thirds of BK_{Ca} channels belong to the scattered pool and about one-third to the clustered pool in principal cell somata. Overall densities of channels in both pools differed in the different cell types analyzed, although being considerably lower compared to cerebellar PC. Postembedding immunogold labeling revealed association of clustered channels with subsurface membrane cisterns and confirmed extrasynaptic localization of scattered channels. This study indicates a common organizational principle for somatic BK_{Ca} channels in central principal neurons with the formation of a clustered and a scattered pool of channels, and a cell-type specific density of this channel type. © 2010 IBRO. Published by Elsevier Ltd.

Key words: BK_{Ca} channel, SDS-FRL, postembedding immunogold electron microscopy, plasmerosome, microdomain, subsurface cistern. Open access under CC BY-NC-ND license.

Large-conductance Ca^{2+} activated potassium channels (also called BK_{Ca}, $K_{Ca}1.1$, Maxi-K, or *Slo1*) are widely distributed in the mammalian brain and play diverse physiological roles in neurons ranging from action potential repolarization to control of cell excitability and neurotransmitter release (Storm, 1987a; Lancaster and Nicoll, 1987; Shao et al., 1999; Hu et al., 2001a; Gu et al., 2007; Hou et al., 2009). They are localized primarily to principal neurons where they are targeted to specific subcellular domains (Knaus et al., 1996; Hu et al., 2001a; Sailer et al., 2006; Misonou et al., 2006). Recently we found that BK_{Ca} channels are distributed non-homogenously in the somato-dendritic plasma membrane of cerebellar Purkinje cells (PC), forming two distinct pools: one pool consisting of channels that are scattered in the extrasynaptic membrane at low density, and the other consisting of channels that cluster in membrane areas overlying subsurface membrane cisterns (SSC; Kaufmann et al., 2009). These two pools of BK_{Ca} channels might differ in function and routes of Ca^{2+} activation.

BK_{Ca} channels ($K_{Ca}1$) form together with the Slack and Slick channels ($K_{Ca}4$) as well as *Slo3* channels ($K_{Ca}5$) the structurally related SLO family of high-conductance Ca^{2+} and Na^{+} activated potassium channels. Small-conductance ($K_{Ca}2$, or SK) and intermediate-conductance Ca^{2+} activated potassium channels ($K_{Ca}3$, or IK) are more distantly related to this family (Wei et al., 2005; Salkoff et al., 2006). BK_{Ca} channels are homotetramers of principal (alpha) subunits, which are products of the KCNMA1 or *Slo1* gene (first cloned in *Drosophila melanogaster*; Adelman et al., 1992). The principal subunits, constituting the pore of the channel, can co-assemble with 1–3 auxiliary beta subunits (KCNMB1-4; Salkoff et al., 2006), which modify the functional properties of the channel in different tissues (Brenner et al., 2000; Sah and Faber, 2002). Alpha subunits show a relatively short extracellular, amino terminal domain (N-terminus) and a large intracellular, carboxyl terminal domain (C-terminus) where the Ca^{2+} binding domain ("calcium bowl") is located (Sah and Faber, 2002; Salkoff et al., 2006). BK_{Ca} channels are distinguished from other potassium channels by their unusually high single-channel conductance (averaging over 250 pS) and being

*Corresponding author. Tel: +43-512-9003-71208; fax: +43-512-9003-73200.
E-mail address: walter.kaufmann@i-med.ac.at (W. A. Kaufmann).

Abbreviations: BK_{Ca}, large-conductance calcium-activated potassium channel; BL, basolateral nucleus of the amygdala; BSA, bovine serum albumin; Ca_V, voltage-gated calcium channel; CICR, calcium induced calcium release; DG, dentate gyrus; ER, endoplasmic reticulum; fAHP, fast afterhyperpolarization; GC, granule cell; IMP, intramembrane particle; K_V, voltage-gated potassium channel; PB, phosphate buffer; PC, Purkinje cell; RT, room temperature; SDS, sodium lauryl sulphate; SDS-FRL, SDS-digested freeze-fracture replica labeling; SSC, subsurface cistern; SSCx, somato-sensory cortex; TBS, tris-buffered saline.

0306-4522/10 © 2010 IBRO. Published by Elsevier Ltd. Open access under CC BY-NC-ND license.
doi:10.1016/j.neuroscience.2010.05.070

gated both by membrane depolarization and changes in cytosolic free [Ca^{2+}] (Salkoff et al., 2006). Increasing $[Ca^{2+}]_i$ shifts the activation curve from highly positive potentials into the physiological voltage range (Cui et al., 1997; Latorre and Brauchi, 2006; Fakler and Adelman, 2008). Yet, BK_{Ca} channels have a low affinity for Ca^{2+}, typically requiring more than 10 μM $[Ca^{2+}]_i$ for activation within physiological membrane potentials (Fakler and Adelman, 2008). The sensitivity of BK_{Ca} channels to Ca^{2+} makes it an important negative-feedback system for Ca^{2+} entry in many cell types, thus regulating transmitter release and other Ca^{2+}-dependent processes (Storm, 1987a, 1990; Hu et al., 2001a).

Activation of BK_{Ca} channels in neurons generates a macroscopic current, which has been called I_C or I_{CT}. This current contributes to action potential repolarization (Lancaster and Nicoll, 1987; Storm, 1987a; Robitaille et al., 1993; Faber and Sah, 2002), mediates an early component of the fast afterhyperpolarization (fAHP; Storm, 1987a; Faber and Sah, 2003), shapes dendritic Ca^{2+} spikes (Golding et al., 1999) and regulates neurotransmitter release at least under certain conditions (Lingle et al., 1996; Hu et al., 2001a; Raffaelli et al., 2004). The diverse functional properties mediated by BK_{Ca} channels (Hou et al., 2009) might be correlated with their differential localization to various subcellar sites and non-homogenous distribution within specific subdomains, as observed in cerebellar PC (Kaufmann et al., 2009). In the present study, we aimed at establishing whether the dual distribution pattern of BK_{Ca} channels found in PC is a general organizational principle for somatic BK_{Ca} channels, common to different types of neurons within different brain areas, rather than being specific to a certain cell type. Hence, we examined BK_{Ca} channel distribution in hippocampal CA3 pyramidal neurons, neocortical layer 5 pyramidal neurons, principal neurons of the central and basolateral amygdaloid nuclei, as well as granule cells of the hippocampal dentate gyrus (DG). All these cell types were shown to express functional BK_{Ca} channels (Brenner et al., 2005; Shao et al., 1999; Benhassine and Berger, 2005; Sausbier et al., 2006; Meis and Pape, 1997) yet their precise subcellular localization has remained unidentified. By means of SDS-digested freeze-fracture replica labeling (SDS-FRL), we performed detailed quantitative analysis of BK_{Ca} channels in the somatic plasma membrane of these cell types (except for principal neurons of the central amygdaloid nucleus) for comparison with respective data in PC (Kaufmann et al., 2009). We also analyzed the subcellular localization of BK_{Ca} channels in DG granule cells by means of thin-section electron microscopy for comparison with PC, since these two cell types show similar membrane specializations like SSC (Le Beux, 1972), but are highly different with respect to the sizes and characteristics of their somata and dendritic trees (Paxinos, 1995), function (excitatory versus inhibitory), and BK_{Ca} channel-related physiological properties (Edgerton and Reinhart, 2003; Sausbier et al., 2004; Brenner et al., 2005).

EXPERIMENTAL PROCEDURES

Materials

Paraformaldehyde, osmium tetroxide, uranyl acetate and pioloform were obtained from Agar Scientific Ltd. (Stansted, UK). EM grade glutaraldehyde was purchased from Polysciences Inc. (Warrington, PA, USA). Thiopental was from Sandoz (Kundl, Austria). Lead (II) citrate was from Merck KGaA (Darmstadt, Germany), picric acid from Fluka GmbH (Buchs, Switzerland). Glycerin and sodium lauryl sulfate (SDS) were from Carl Roth GmbH (Karlsruhe, Germany). Normal goat serum was from Bender (Vienna, Austria), bovine serum albumin (BSA) from Serva (Heidelberg, Germany). Gold-conjugated immunoglobulins were from British BioCell Int. (Cardiff, UK). Eukitt was from Kindler (Freiburg, Germany). Platinum and carbon rods were from Bal-Tec (Balzers, Liechtenstein). Lowicryl HM20 resin and all remaining chemicals were from Sigma-Aldrich (Vienna, Austria).

Antibody production and specification

BK_{Ca} channel antibodies were produced and kindly provided by Hans-Guenther Knaus (Department Medical Genetics, Molecular and Clinical Pharmacology, Innsbruck Medical University, Austria). In brief, antibodies were affinity purified from immune sera raised in rabbit using immunogenic peptides designed from the mouse *Slo1* sequence, containing residues 913–926 [anti-BKα (913–926)] (Knaus et al., 1995) and residues 1118–1132 [anti-BKα (1118–1132)] (Wanner et al., 1999). Both sequences show 100% homology between rat and mouse. Antibodies were characterized by enzyme-linked immunosorbent assay, immunoprecipitation and immunoblotting. The antibodies recognized single bands of approximately 125 kDa in immunoblot analysis of rat and mouse whole-brain membranes (Knaus et al., 1996; Sausbier et al., 2004). Specificity of these antibodies was tested and confirmed by immunocytochemistry in light microscopy (Grunnet and Kaufmann, 2004; Sailer et al., 2006) and in electron microscopy (Hu et al., 2001a; Kaufmann et al., 2009). In the present study, both antibodies were used for SDS-FRL as well as post-embedding immunogold cytochemistry and yielded identical results. Specificity of immunolabeling was confirmed on tissue samples from BK_{Ca} channel null mice, kindly provided from Peter Ruth (Institute of Pharmacy, University of Tuebingen, Germany).

Anti-mSlo maxi-K^+ channel. A monoclonal anti-BK_{Ca} channel antibody was obtained from the UC Davis/NIH NeuroMab Facility, supported by NIH grant U24NS050606 and maintained by the Department of Neurobiology, Physiology and Behavior, College of Biological Sciences, University of California, Davis, CA 95616, USA (Cat.No. 75-022). The antibody was produced against a fusion protein corresponding to amino acids 690–1196 of mouse *Slo1* (clone L6/60) and recognized a single band of approximately 125 kDa in immunoblot analysis of rat hippocampal membrane preparations. In the present study, the antibody was applied successfully in post-embedding immunogold labeling yielding same results as anti-BKα (913–926) and anti-BKα (1118–1132). Specificity of immunolabeling was tested and confirmed on tissue samples from BK_{Ca} channel null mice.

Animals and tissue preparation

Immunochemical studies were performed on samples from adult male Sprague–Dawley rats (250–300 g; Department Laboratory Animals and Genetics, Medical University, Vienna, Austria), adult male C57Bl/6 mice (10–12 weeks; Medical University, Vienna, Austria) and adult male BK_{Ca} channel null mice (10–12 weeks; Sausbier et al., 2004). All experimental protocols were approved by the Animal Experimentation Ethics Board, in compliance with both, the European Convention for the Protection of Vertebrate Animals used for Experimental and Other Scientific Purposes

(ETS no. 123) and the European Communities Council Directive of November 24, 1986 (86/609/EEC). The authors further attest that all efforts were made to minimize the number of animals used and their suffering. Animals were deeply anesthetized by intraperitoneal injection of thiopental (12 mg/100 g body weight) and perfused transcardially with phosphate buffered saline (PBS; 25 mM, 0.9% NaCl, pH 7.4) followed by chilled fixative (buffer conditions are given below for the different techniques used). After fixation, brains were removed from the skull immediately, washed in phosphate buffer (PB; 0.1 M, pH 7.4) and stored in 0.1 M PB containing 0.05% sodium azide at 4 °C.

SDS-digested freeze-fracture replica labeling (SDS-FRL)

SDS-FRL was performed with some modifications to the original method (Fujimoto, 1995; Masugi-Tokita et al., 2007). The experimental animals ($n=15$: five Sprague–Dawley rats, five C57Bl/6 mice, and five BK_{Ca} channel null mice) were perfusion fixed with PB (0.1 M, pH 7.4) containing 1% formaldehyde and 15% of a saturated solution of picric acid. The brains were removed from the skull immediately and forebrains were cut into 140 μm coronal sections with a Vibroslicer (VT1000S; Leica Microsystems, Vienna Austria). Samples were dissected from respective brain areas and cryoprotected with 30% glycerol in 0.1 M PB overnight at 4 °C. Samples were then frozen by use of a high-pressure freezing machine (HPM 010; Bal–Tec, Balzers, Liechtenstein) and fractured by a double replica method in a freeze-etching device (BAF 060; Bal–Tec). Fractured faces were replicated by evaporation of carbon (rotating) by means of an electron beam gun positioned at a 90° angle to a thickness of 5 nm and shadowed unidirectionally with platinum-carbon at a 60° angle (thickness 2 nm). Finally, a 15 nm thick layer of carbon was applied from a 90° angle (rotating). Tissue was solubilized in a solution containing 2.5% SDS and 20% sucrose made up in 15 mM Tris buffer, pH 8.3, on a shaking platform for 18 h at 80 °C. Replicas were kept in the same solution at room temperature until they were processed further.

On day of immunolabeling, replicas were washed in Tris-buffered saline (TBS; 50 mM, 0.9% NaCl, pH 7.4) containing 0.05% BSA and incubated in a blocking solution containing 5% BSA in 50 mM TBS for 1 h at room temperature (RT). Subsequently, the replicas were incubated in the primary antibody diluted in the same solution as described above, overnight at 7 °C. Dilution of antibodies used was: anti-BKα (913–926) 1.8 μg/ml; anti-BKα (1118–1132) 2 μg/ml. After several washes in TBS, the replicas were reacted with gold-conjugated goat anti-rabbit secondary antibodies made up in 50 mM TBS (1:30) containing 5% BSA overnight at 7 °C. They were then washed in double-distilled water, mounted on formvar-coated 100-line copper grids and analyzed in a Philips CM120 TEM equipped with a Morada CCD camera (Soft Imaging Systems, Münster, Germany). Whole images were level adjusted, sharpened, and cropped in Photoshop (Adobe) without changing any specific features within. The specificity of the immunolabeling was controlled and confirmed applying the respective pre-immune serum, applying the immune serum preadsorbed with the synthetic immunogenic peptides (concentration 10 μM), and applying the immune serum on samples from BK_{Ca} channel null mice, respectively.

Sampling and analysis of SDS-FRL data. Five to seven replicas were used for quantification of BK_{Ca} channel immunolabeling per respective brain area, which were: somatosensory cortex, field CA3 of hippocampus, DG, and basolateral nucleus of the amygdala (BL). Within these areas, aspects of principal cells were selected at random and electron micrographs were taken at a magnification of $\times$43,000–$\times$125,000. The magnification was verified by use of a calibration grid. Clusters of more than nine intramembrane particles (IMP) labeled with more than three immunogold particles were considered BK_{Ca} immunoreactive clusters. The outline of clusters was demarcated by hand, and immunogold particles within 20 nm from the cluster edge were included in the analysis since particles can be as distant from the respective epitope (Matsubara et al., 1996). Quantification was performed by means of AnalySIS (Soft Imaging Systems), and data were expressed as mean$\pm$SD. Statistical analysis was carried out in Prism (GraphPad Software, Inc.). Group comparisons were performed by 1way ANOVA followed by post hoc Bonferroni's multiple comparison tests ($\alpha=0.05$).

For estimating the total number of immunoparticles labeling BK_{Ca} channels per DG granule cell soma, as well as the ratio of BK_{Ca} channels in the scattered and the clustered pool of channels, the surface of an average granule cell soma was calculated considering it as a spheroid (prolate ellipsoid) with a height=18 μm and width=10 μm; these values were based on specifications from Amaral and Witter (1995).

Postembedding immunogold labeling

The experimental animals ($n=15$: five Sprague–Dawley rats, five C57Bl/6 mice, and five BK_{Ca} channel null mice) were perfusion fixed with PB (0.1 M, pH 7.4) containing 4% formaldehyde and 0.05% glutaraldehyde. The brains were taken out and respective tissue blocks were dissected, freeze-substituted and embedded at low temperature in Lowicryl HM20 resin (Takumi et al., 1999). Ultrathin sections (70–80 nm) were cut on a Leica ultramicrotome (Ultracut S; Leica, Vienna, Austria), mounted on formvar-coated nickel mesh grids, and processed for immunogold cytochemistry (Matsubara et al., 1996). Sections were etched with 1% H_2O_2 in TBS for 20 min at RT, followed by incubation in 50 mM glycine in TBS containing 0.1% Triton X-100 (TBS-T; pH 7.4) for 10 min at RT. After application of 2% BSA, 2% normal goat serum and 0.2% milk powder in TBS-T for 20 min to block non-specific binding sites, sections were incubated with primary antibodies diluted in TBS-T containing 2% BSA overnight at 7 °C. Concentration of antibodies used were: affinity purified anti-BKα (913–926) 1.8 μg/ml; anti-BKα (1118–1132) 2.4 μg/ml; anti-mSlo maxi-K^+ channel 2.2 μg/ml. After rinsing in TBS-T (four times 10 min each), gold-conjugated goat anti-rabbit or goat anti-mouse antibodies, respectively, were applied (diluted 1:30 in TBS-T containing 2% BSA and 0.05% polyethylene glycol; for 90 min at RT). The sections were then rinsed in double-distilled water and air-dried. The sections were stained with Uranyl Acetate and Lead Citrate and examined in a TECNAI G^2 as well as a Philips CM120 TEM, both equipped with a Morada CCD camera. Whole images were level adjusted, sharpened, and cropped in Photoshop (Adobe) without changing any specific features within. Specificity of immunolabeling was controlled and confirmed by applying the respective pre-immune serum, applying antibodies preadsorbed with excess immunogenic peptides (concentration 10 μM), and applying antibodies on sections from samples of BK_{Ca} channel null mice.

Sampling and analysis of postembedding immunogold data. Five samples were taken at random from the DG granule cell layer of the rat dorsal hippocampus (approximate anteroposterior level -3.4 mm; Paxinos and Watson, 1998), and four sections were analyzed per sample. Electron micrographs were taken at a magnification of $\times$43,000. The magnification was verified by use of a calibration grid, nonspecific immunolabeling was determined in preadsorption experiments. To establish the subcellular distribution profile of immunogold particles, the distance of particles perpendicular to the inner leaflet of the somatic plasma membrane was analyzed within a range of 25 nm toward the extracellular side (indicated with negative values) and 200 nm toward the cell interior ($n=500$). Quantification was performed by means of AnalySIS (Soft Imaging Systems), and data were expressed as mean$\pm$SD. For the comparison of the BK_{Ca} channel distributions in areas of the plasma membrane with and without underlying SSC, the sub-

cellular particle distribution was established for each of the areas perpendicular to the inner leaflet of the plasma membrane within a range of 25 nm toward the extracellular side (indicated with negative values) and 80 nm toward the cell interior (n=200 particles each).

RESULTS

Two pools of somatic BK_{Ca} channels in principal neurons of the central nervous system: clustered and scattered channels

The somatic localization and spatial distribution of BK_{Ca} channels were studied by means of SDS-FRL in a subset of central principal neurons, namely in hippocampal pyramidal cells, DG granule cells, neocortical layer 5 pyramidal cells and principal cells of the central as well as basolateral nuclei of the amygdala. The SDS-FRL technique allows localization and density analysis of integral membrane proteins beyond limitations of thin-section electron microscopy. Freeze-fracturing and replication of membrane leaflets, with subsequent solubilization of unfractured tissue constituents facilitate the view of large areas of the plasma membrane which are also accessible to antibody binding without diffusion restrictions.

We found that BK_{Ca} channels form two distinct pools in the somatic plasma membrane of all cell types analyzed, although at different densities. All cell types showed both scattered channels and clusters of channels. Such a dual distribution pattern was seen specifically in layer 5 pyramidal neurons of the somatosensory cortex (SSCx; Fig. 1A, B), hippocampal CA3 pyramidal neurons (Fig. 1C, D), principal neurons of the basolateral (BL; Fig. 1E) as well as central amygdaloid nuclei (Fig. 1F), and hippocampal DG granule cells (Fig. 2A–H). These findings indicate that a separation into two distinct pools of channels, which we found for the first time in cerebellar PC (Kaufmann et al., 2009), is likely to represent a common organizational pattern for BK_{Ca} channels in the soma of central principal neurons.

Different densities of clustered and scattered BK_{Ca} channels

Detailed quantitative analysis of BK_{Ca} channel densities was performed in DG granule cells, CA3 pyramidal neurons, layer 5 pyramidal neurons of the SSCx, and principal neurons of the BL (Table 1). With respect to the abundance of clustered channels, large differences were observed in immunoparticle densities within clusters ranging from 102±14 particles per μm^2 membrane in BL principal neurons to 175±24 particles per μm^2 membrane in CA3 pyramidal neurons (total number of clusters analyzed in each cell type=40). The average number of particles per cluster was similar in DG granule cells, SSCx pyramidal neurons and BL principal neurons with about eight particles per cluster. Compared to these cell types, the average number of particles per cluster was significantly higher in CA3 pyramidal neurons ($P<0.001$) with about 12 particles per cluster. The density of clusters per area of somatic plasma membrane was similar in all four cell types with about one cluster per 13 μm^2 membrane (total membrane area analyzed in each cell type=600 μm^2). Significant difference in cluster density was only observed for DG granule cells compared to CA3 pyramidal neurons (5.8±1.8 versus 9.2±3.7 clusters per 100 μm^2 membrane, respectively; $P<0.01$). Also the average size of clusters (≈0.07 μm^2) was similar in the four cell types, and no significant difference in cluster size was observed.

For the second pool of immunoparticles labeling BK_{Ca} channels scattered in the somatic plasma membrane (Fig. 2E, G), the density was considerably lower compared to that within clusters, and differed largely in the cell types analyzed (Table 1). In DG granule cells and CA3 pyramidal neurons, about one immunoparticle was detected per 1.0 μm^2 of plasma membrane, whereas in SSCx pyramidal neurons and BL principal neurons, a significantly minor density was seen with about 1 particle per 1.4 μm^2 plasma membrane ($P<0.001$; total membrane area analyzed in each cell type=250 μm^2; background levels established in BK_{Ca} channel null mice=0.26±0.03 particles per μm^2 membrane).

We then compared the density of somatic BK_{Ca} channels in the four cell types to that established for cerebellar PC (Kaufmann et al., 2009). With respect to the clustered pool, the average size of clusters, particle density within clusters, and average number of particles per cluster were all significantly larger in PC ($P<0.001$). Noteworthy, the density of clusters per unit membrane area was instead comparable between most cell types, with the only exception of DG granule cells, which showed a considerably lower density of clusters compared to PC and CA3 pyramidal neurons (Table 1). With respect to the scattered pool, the density of immunoparticles was significantly higher in PC compared to all other cell types (ratio of particle density in PC to other cell types ≈6:1; Table 1).

To estimate the ratio of scattered to clustered BK_{Ca} channels in the soma of a central principal model neuron, we calculated the total number of immunoparticles labeling BK_{Ca} channels for both pools in DG granule cells, since this cell type exhibits cell bodies of relatively homogeneous dimensions with a smooth surface membrane (Laatsch and Cowan, 1966; Amaral and Witter, 1995). In this cell type, we detected about one cluster of immunoparticles per 17 μm^2 of somatic plasma membrane (5.8±1.8 clusters per 100 μm^2 membrane). Considering the total surface area of an average granule cell soma as 648 μm^2 (see Experimental Procedures), this yields approximately 38 clusters per soma. Since 8.5 particles were detected per average cluster, this results in about 323 particles per DG granule cell soma in the clustered pool. The density of scattered particles was 0.98±0.21 particles per μm^2 somatic plasma membrane. This yields about 635 particles per granule cell soma in the scattered pool, that is almost twice as many particles as in the clustered pool. Thus, presuming a similar labeling efficacy for both pools of channels, about two-thirds of BK_{Ca} channels in an average principal cell soma would belong to the scattered pool and about one-third to the clustered pool.

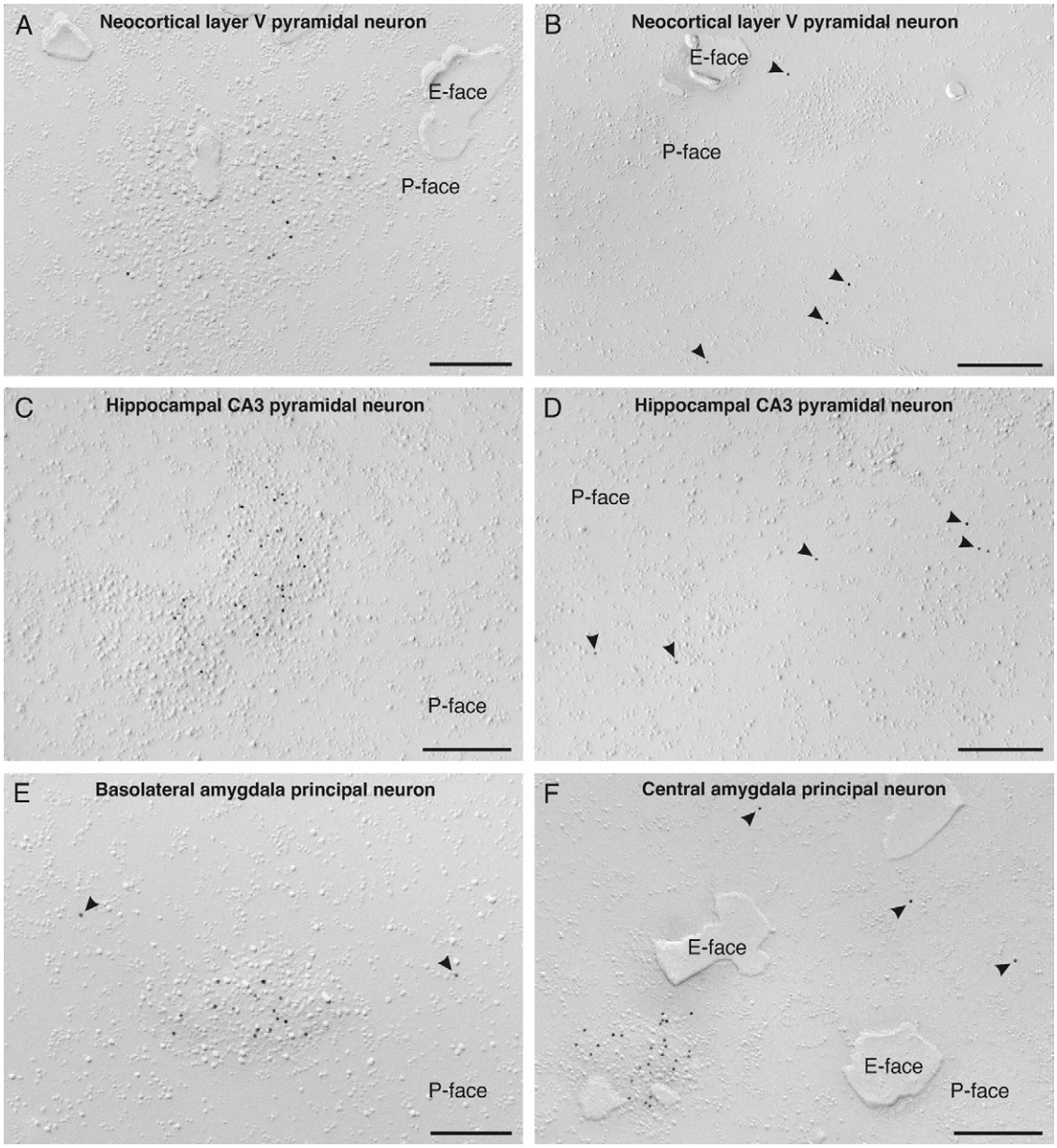

Fig. 1. Localization of BK_{Ca} channels in the somatic plasma membrane of central principal neurons revealed with SDS-digested freeze-fracture replica labeling in rat brain. (A) A high-power photograph of an aspect of the somatic plasma membrane of a layer V pyramidal neuron of the somato-sensory cortex reveals a cluster of immunolabeled BK_{Ca} channels associated with a cluster of intramembrane particles (IMPs). Antibodies conjugated to 10 nm gold particles and directed against epitopes at an intracellular C-terminal domain of the α subunit (anti-BKα, residues 913–926) were applied, thus labeling is detected in the P-face of the plasma membrane. The E-face is free of any immunolabeling. (B) In the same pyramidal neuron, scattered BK_{Ca} channels are detected in the P-face of the somatic plasma membrane indicated with an arrowhead. (C) Clustering of BK_{Ca} channels, associated with clusters of IMPs, is also observed in the somatic plasma membrane P-face of a hippocampal CA3 pyramidal neuron. The density of immunolabeling is higher as in the neocortical pyramidal neuron, shown in (A). (D) Scattered immunoparticles (arrowheads) are observed in the P-face of the CA3 pyramidal neuron too. (E) Clustered and scattered BK_{Ca} channels (the latter are indicated with an arrowhead) were also found in the plasma membrane P-face of a principal neuron of the basolateral amygdaloid nucleus. (F) The same distribution pattern of BK_{Ca} channels with clustered and scattered channels (arrowheads) is observed in the plasma membrane P-face of a principal neuron of the central amygdaloid nucleus. The E-face is free of any immunolabeling. Scale bar=200 nm in (A, E); 300 nm in (B); 275 nm in (C, F); 250 nm in (D).

Clustered BK_{Ca} channels are associated with plasma membrane domains overlying SSC

Since we observed that clustered BK_{Ca} channels were always associated with SSC in cerebellar PC using thin section electron microscopy (Kaufmann et al., 2009), we thus analyzed (i) the cyto-architecture beneath domains of the plasma membrane enriched in BK_{Ca} channels in DG granule cells, and studied (ii) possible localization of BK_{Ca} channels to intracellular organelles. We have chosen DG granule cells for this analysis since SSC are distinct and well described in this cell type (Laatsch and Cowan, 1966;

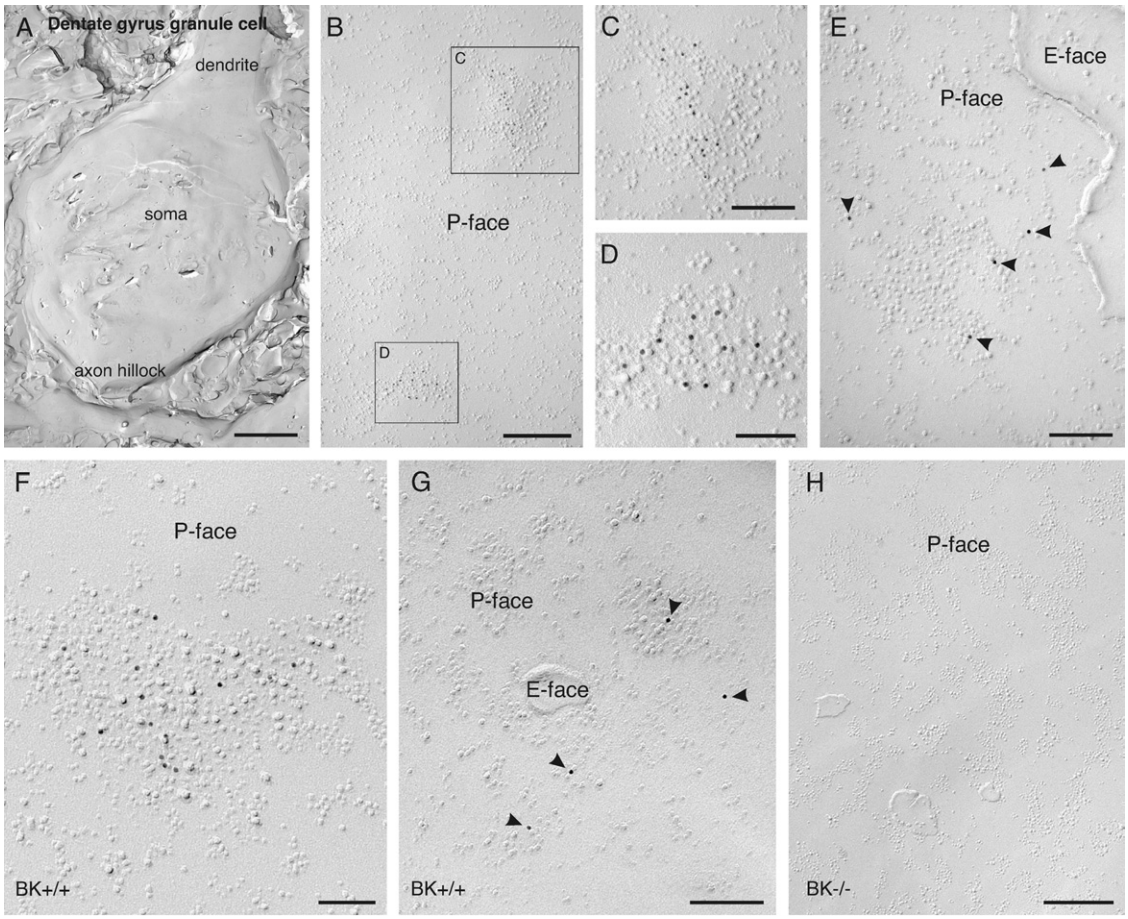

Fig. 2. Clustered and scattered BK_{Ca} channels in the somatic plasma membrane of DG granule cells detected with SDS-digested freeze-fracture replica labeling in rat (A–E) and mouse brain (F–H). (A) A low-power photograph shows a large aspect of a granule cell soma, including the very proximal portion of the principal dendrite and the axon hillock. (B) A high-power photograph of an aspect of the granule cell somatic plasma membrane shows the distribution of BK_{Ca} channels in the P-face of the somatic plasma membrane. Antibodies conjugated to 10 nm gold particles and directed against epitopes at the intracellular C-terminal end of the α subunit were applied. (C, D) Clusters of immunoparticles labeling BK_{Ca} channels in the plasma membrane are associated with clusters of IMPs (aspects of the plasma membrane at higher magnification, indicated by a boxed area in B). (E) Some immunoparticles labeling BK_{Ca} channels are scattered in the plasma membrane P-face (indicated with an arrowhead). The E-face of the plasma membrane is free of any immunolabeling. (F, G) The same distribution pattern of BK_{Ca} channels is observed in the plasma membrane of DG granule cell somata in mouse (C57Bl/6; BK+/+), with a clustered (F) and a scattered (G) pool of channels in the plasma membrane P-face. (H) Antibody specificity is controlled and confirmed in replicas of BK_{Ca} channel null mice (BK−/−). Scale bar=2.75 μm in (A); 350 nm in (B, D, H); 175 nm in (C); 150 nm in (E, G); 100 nm in (F).

Kolde and Themann, 1982). We applied post-embedding immunogold labeling on freeze-substituted and Lowicryl embedded ultra-thin sections (van Lookeren Campagne et al., 1991). This method holds the advantage of high spatial resolution in the subcellular dimension, although at cost of labeling sensitivity.

Consistent with our findings in SDS-FRL, also post-embedding immunogold labeling revealed two pools of BK_{Ca} channels in the plasma membrane of DG granule cells: one pool of scattered channels and a second pool of clustered channels in the somatic plasma membrane (Fig. 3A–H). Clustering of BK_{Ca} channels was exclusively observed in areas of the plasma membrane overlying SSC (Fig. 3B, F). In DG granule cells, SSC are usually formed by a 0.5–1.0 μm long outer cistern of the endoplasmic reticulum (ER), free of ribosomes. These cisterns run in parallel to the inner leaflet of the plasma membrane at a regular distance of about 9–13 nm and usually widen at their lateral edges. One (Fig. 3B) or two inner cisterns of rough ER can be closely apposed at a distance of 30–40 nm from the superficial cistern and from each other (Le Beux, 1972; Kolde and Themann, 1982).

Outside these clusters, scattered immunoparticles labeling BK_{Ca} channels were regularly observed in the extrasynaptic plasma membrane (Fig. 3D, G). Postsynaptic membrane specializations of axo-somatic synapses (symmetric, Gray's type II synapses; Laatsch and Cowan, 1966) were free of BK_{Ca} channel immunolabeling (Fig. 3E). Specificity of immunolabeling was tested and confirmed in sections of BK_{Ca} channel null mice (Fig. 3H). For establishing the abundance of scattered channels, the linear density of immunoparticles was established along the somatic plasma membrane. Portions of the somatic plasma membrane were randomly selected (aside from

Table 1. Density of clustered and scattered immunoparticles labeling BK_{Ca} channels in the soma of dentate gyrus granule cells (GC), hippocampal CA3 pyramidal neurons (CA3), layer V pyramidal neurons of the somatosensory cortex (SSCx) and principal neurons of the basolateral amygdala (BL) compared to cerebellar Purkinje cells (PC¥; values for PC were published by Kaufmann et al., 2009)

	GC	CA3	SSCx	BL	PC¥
Average size of a cluster (in μm^2; $n=40$)	0.069±0.013 ***	0.071±0.011 ***	0.070±0.019 ***	0.073±0.014 ***	0.151±0.036
Particle density within a cluster (in particles per μm^2; $n=40$)	124±14 †††,###,***	175±24 ‡‡‡,###,***	114±29 ***	102±15 ***	341±31
Number of particles per cluster (in particles per cluster; $n=40$)	8.5±1.6 †††,***	12.4±2.3 ‡‡‡,###,***	7.8±2.2 ***	7.4±2.6 ***	46.8±4.9
Density of clusters (in clusters per 100 μm^2; area=600 μm^2)	5.8±1.8 ††,**	9.2±3.7	7.5±2.1	8.1±3.0	9.5±2.2
Density of scattered particles (in particles per μm^2; area=250 μm^2)	0.98±0.21 ‡‡‡,##,***	1.03±0.26 ‡‡‡,###,***	0.67±0.12 ***	0.74±0.17 ***	5.68±0.43
Background levels (in particles per μm^2; area=250 μm^2)	0.26±0.03	n.d.	n.d.	n.d.	0.32±0.18

n.d., not determined.

Group comparisons were performed by 1 way ANOVA followed by post hoc Bonferroni's ($\alpha=0.05$): †, GC versus CA3; ‡, GC versus SSCx; #, GC versus BL; ∗, GC versus PC; ‡, CA3 versus SSCx; #, CA3 versus BL; ∗, CA3 versus PC; #, SSCx versus BL; ∗, SSCx versus PC; ∗, BL versus PC; $P<0.01$, two symbols; $P<0.001$, three symbols.

areas overlying SSC) and all particles within a range of ±20 nm to the inner leaflet of the plasma membrane were sampled. Post-embedding immunogold labeling techniques are based on indirect immunodetection of antigens and hence, the localization of immunoparticles does not directly represent the localization of the epitope. Specifically, gold particles may be as far as 20 nm from its epitope because of the size of the interposed immunoglobulins, the Fab' fragments, and the size of the gold particles themselves (Matsubara et al., 1996). This analysis revealed a density of 0.35±0.08 particles per μm extrasynaptic plasma membrane (total length analyzed=60 μm). The density of particles within postsynaptic specializations of axo-somatic synapses was 0.19±0.05 particles per μm membrane (number of synapses analyzed=40). The densities in post-synaptic specializations are close to background levels established in samples of BK_{Ca} channel null mice (0.15±0.04 particles per μm membrane; total length analyzed=80 μm), indicating a lack of BK_{Ca} channel localization in postsynaptic membrane specializations of the soma.

BK_{Ca} channels are mainly integrated in the plasma membrane

In order to analyze possible localization of BK_{Ca} channels to intracellular organelles in addition to the plasma membrane, we established a vertical frequency profile of immunogold particles along an axis perpendicular to the somatic plasma membrane. The inner leaflet of the plasma membrane was used as reference line, and the vertical distribution of gold particles was analyzed within a range of 25 nm toward the extracellular side and 200 nm toward the cell interior. Portions of DG granule cell somata were randomly selected, and all gold particles within the given range were analyzed and binned in 5 nm intervals. This plot revealed a peak corresponding with the plasma membrane, indicating that the majority of the immunosignal originated from plasma membrane labeling (Fig. 4A). Of all particles analyzed ($n=500$), 71.4% were localized within a range of ±20 nm from the inner leaflet of the plasma membrane. However, the distribution profile was not exactly Gaussian, but appeared slightly skewed toward the cell interior. This inward skew seems too large to being fully explained by the localization of the epitope in the cytoplasmic domain of the alpha subunit. It indicates that small subpopulations of BK_{Ca} channels may be localized to intracellular organelles, in addition to the main population of channels in the plasma membrane.

To establish whether a BK_{Ca} channel subpopulation could be localized to junctional ER components like SSC, we re-analyzed the vertical frequency profile of immunogold particles with respect to (i) areas of the plasma membrane with SSC lying beneath it and (ii) areas of the plasma membrane outside SSC without any visible ER beneath it. Gold particles were sampled within a range of 20 nm toward the extracellular side and 75 nm toward the cell interior ($n=200$ particles, each) along an axis perpendicular to the inner leaflet of the plasma membrane used as reference line. In areas of the plasma membrane outside SSC, the particle distribution appeared approximately Gaussian with the peak coinciding with the plasma membrane. This re-affirms that BK_{Ca} channels are primarily localized in the plasma membrane (Fig. 4B). Conversely, in areas of the plasma membrane with underlying SSC, the distribution profile showed a peak coinciding with the plasma membrane and a small shoulder at a distance of about 10–20 nm toward the cell interior. This may indicate a small subpopulation of BK_{Ca} channels being localized in SSC, in addition to the main population of channels in the plasma membrane (Fig. 4B).

DISCUSSION

Two pools of somatic BK_{Ca} channels in principal neurons of the central nervous system

Our ultra-structural investigations revealed two pools of BK_{Ca} channels in the somata of central principal neurons–one pool consisting of clustered and another of scattered channels in the extrasynaptic plasma membrane. This

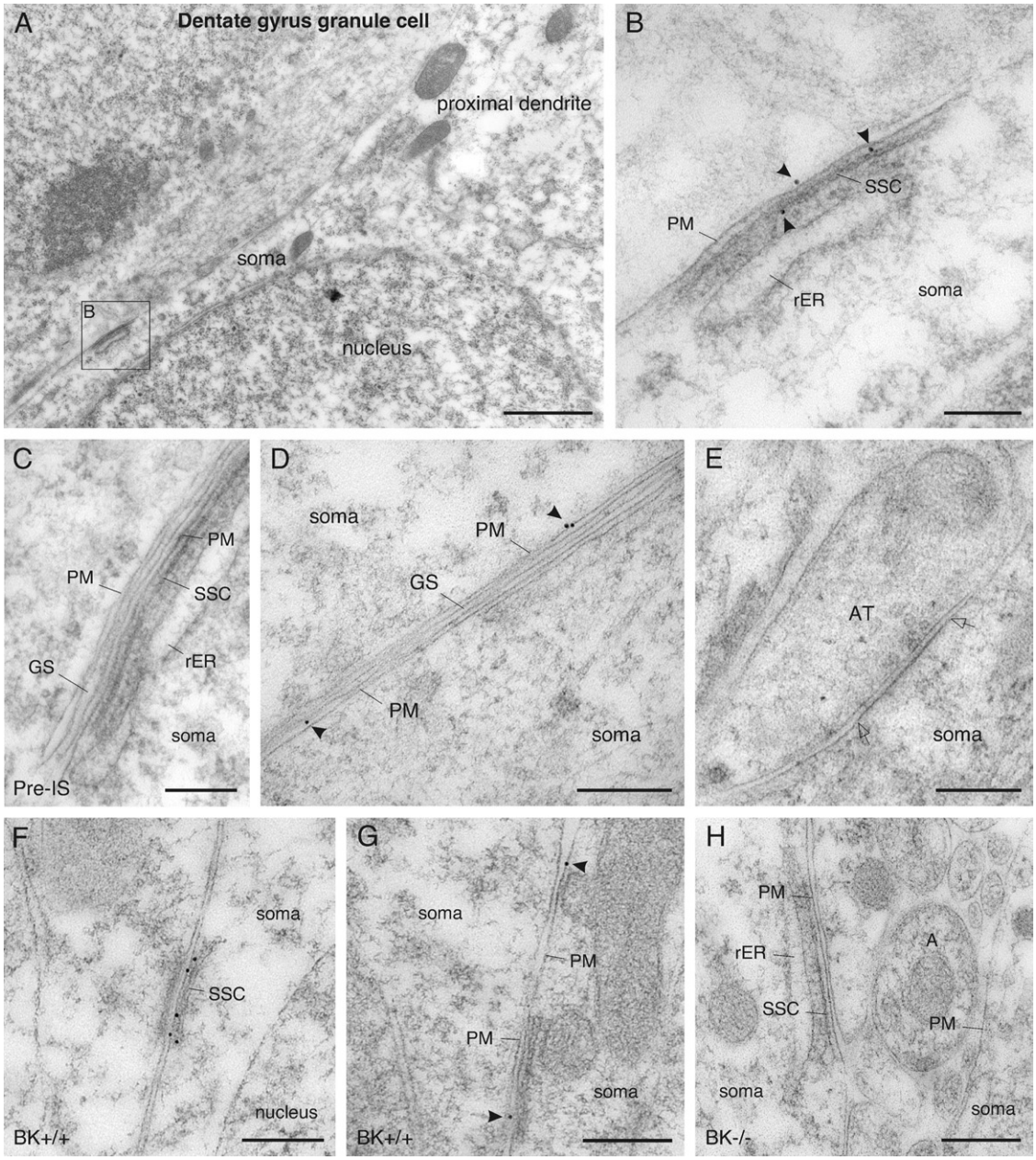

Fig. 3. Localization of BK_{Ca} channels in dentate gyrus granule cell somata of rat (A–E) and mouse brain (F–H) revealed by post-embedding immunogold labeling. Antibodies conjugated to 10 nm gold particles were applied on Lowicryl embedded ultra-thin sections. (A) A low-power micrograph shows an aspect of a granule cell soma and the very proximal portion of the raising principal dendrite. (B) Immunoparticles labeling BK_{Ca} channels are clustered in areas of the somatic plasma membrane with underlying subsurface cisterns (boxed area in A; immunoparticles are indicated with an arrowhead). (C) Specificity of immunolabeling in rat tissue is tested and confirmed by applying the respective pre-immune serum. (D) Outside areas of the plasma membrane with underlying subsurface cisterns, immunoparticles are scattered in the extrasynaptic plasma membrane with low abundance (arrowheads). (E) The postsynaptic membrane specialization of symmetric, presumably inhibitory synapses, is free of BK_{Ca} channel immunolabeling (margins of the postsynaptic membrane specialization are indicated with open arrows). (F) As in the rat, clustering of BK_{Ca} channels in areas of the plasma membrane with underlying subsurface cisterns is seen in the granule cell soma of mouse (C57Bl/6; BK+/+). (G) Outside these areas, scattered immunoparticles are localized in the extrasynaptic plasma membrane with low abundance (arrowheads). (H) Specificity of immunolabeling is tested and confirmed in sections of BK_{Ca} channel null mice (BK−/−). A, axonal profile; AT, axon terminal; GS, glial sheath; PM, plasma membrane; Pre-IS, pre-immune serum; rER, rough endoplasmic reticulum; SSC, subsurface cistern. Scale bar=1.5 μm in (A); 200 nm in (B, D, G); 250 nm in (C, E, H); 500 nm in (F).

characteristic distribution pattern of somatic BK_{Ca} channels was observed in all types of neurons examined, specifically in cortical layer 5 pyramidal neurons, hippocampal CA3 pyramidal neurons, principal neurons of the central as well as basolateral amygdaloid nuclei, and DG granule cells. Recently, we reported a similar non-homogeneous distribution for BK_{Ca} channels in the soma of cerebellar PC (Kaufmann et al., 2009). Thus, the formation of a clustered

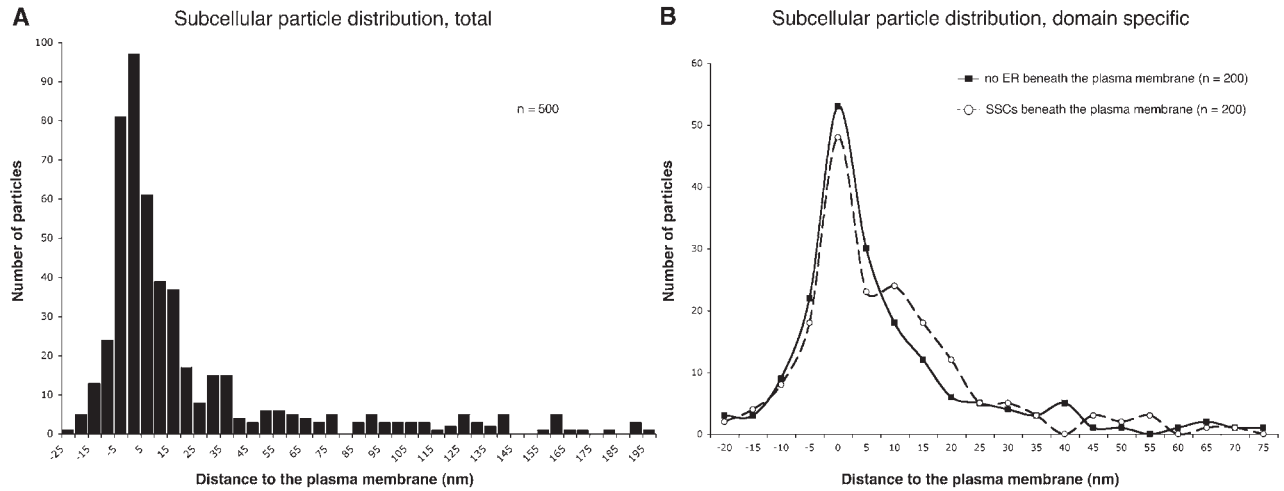

Fig. 4. Subcellular distribution profile of gold particles labeling BK_{Ca} channels [anti-BKα (913–926); 10 nm gold] assessed along an axis perpendicular to the inner leaflet of the somatic plasma membrane of rat dentate gyrus granule cells. (A) The distribution profile (n=500, binning=5 nm) was analyzed within a range of 25 nm toward the extracellular side (indicated with negative values) and 200 nm toward the cell interior. Zero is defined as the center of the inner membrane leaflet. The distribution profile is peaking over the plasma membrane with the mode slightly skewed toward the cell interior. (B) The subcellular particle distribution was reanalyzed and compared in areas of the somatic plasma membrane with underlying subsurface membrane cisterns and in areas of the plasma membrane without visible endoplasmic reticulum (ER) lying beneath it. Particles within a range of 20 nm toward the extracellular side (indicated with negative values) and 75 nm toward the intracellular side were included in this analysis. Zero is defined as the center of the inner membrane leaflet. The particle distribution in areas of the plasma membrane without visible ER beneath it (solid line; n=200 particles, binning=5 nm) shows a Gaussian-shaped distribution profile peaking over the plasma membrane. In areas of the plasma membrane with underlying subsurface cisterns, the particle distribution (dashed line; n=200, binning=5 nm) displays a prominent peak at the level of the plasma membrane and a small shoulder at an interval of about 10–25 nm toward the cytoplasmic side.

and a scattered pool of BK_{Ca} channels seem to represent a common organizational principle for somatic BK_{Ca} channels in principal neurons of different parts of the mammalian brain. The two pools of channels are likely independent from each other, although switching between both pools may play a role as it was shown for neurotransmitter receptors migrating between synaptic and extrasynaptic membranes (Triller and Choquet, 2005).

Different densities of clustered and scattered BK_{Ca} channels in different cell types

Despite the common organizational principle in somatic BK_{Ca} channels with a clustered and a scattered pool, we found striking differences between different cell types regarding the densities of BK_{Ca} channels, and such differences were found for both channel pools. Noteworthy, cerebellar PC seem to constitute a class of their own with respect to BK_{Ca} channel densities (Kaufmann et al., 2009). Their massive BK_{Ca} channel clusters stand out against those of all the other cell types, both in terms of size and channel density within a cluster. In PC, the number of immunoparticles labeling BK_{Ca} channels per cluster is on average 3.8–6.3 times than that of the other cell types. The difference in density of scattered immunoparticles is even more evident, and 5.5–8.5 times higher in PC than in any of the other cells.

Why do cerebellar PC have so much higher BK_{Ca} channel densities than the others? PC have a larger cell body (Amaral and Witter, 1995), are neurochemically different since being GABAergic (Paxinos, 1995), and the duration of their action potential is far briefer than in any of the other cell types examined (Hu and Storm, 2001b; Edgerton and Reinhart, 2003; Sausbier et al., 2004; Brenner et al., 2005). The most striking difference in all measured properties, however, is between cerebellar PC and DG granule cells. The large difference in channel density might be represented functionally by the considerable difference in action potential duration, or more specifically, in the different speed of spike repolarization. The action potential in PC is much briefer than in DG granule cells, the spike duration at half amplitude being only ~0.2 ms versus ~0.7–1.2 ms (at ~32–34 °C), respectively (Geiger and Jonas, 2000; Hu and Storm, 2001b; Edgerton and Reinhart, 2003; Sausbier et al., 2004; Brenner et al., 2005). Despite BK_{Ca} channels may play just a minor role in spike repolarization in either of these cell types (Geiger and Jonas, 2000; Hu and Storm, 2001b; Womack and Khodakhah, 2002; Edgerton and Reinhart, 2003; Sausbier et al., 2004; Brenner et al., 2005), it can be surmised that higher channel densities are needed to generate faster spikes, because a larger current is required to charge the membrane capacitance more rapidly. Specifically, rapid spike repolarization requires high densities of repolarizing potassium channels. Since PC spikes repolarize extremely rapidly, likewise many other GABAergic neurons, they may need a large BK_{Ca} current and hence a high channel density for contributing appreciably to spike repolarization. However, spike repolarization might depend primarily on the activity of voltage-gated potassium (K_V) channels.

Somatic BK_{Ca} channels seem to be needed mainly for generating a fAHP that contributes to recovery of sodium channels from inactivation during interspike intervals thus

allowing high-frequency firing (Sausbier et al., 2004). In order to activate a sufficient BK_{Ca} channel current to produce an efficient fAHP, a larger number of BK_{Ca} channels is needed in a cell with brief spikes (i.e. cerebellar PC) than in a cell with more long-lasting spikes (i.e. DG granule cells), since a briefer spike will activate a smaller fraction of available channels, again assuming that other factors are equal. Although this may be a main reason for the large difference in the overall density of somatic BK_{Ca} channels, it is unlikely that all other factors are in fact equal. Obviously, the opening kinetics of the BK_{Ca} channels themselves, the nature of the specific Ca^{2+} source and the speed as well as efficiency in the coupling with the Ca^{2+} source are important factors that may differ between the two cell types. Since cerebellar PC are also substantially larger than DG granule cells, their far larger surface area and, hence, larger membrane capacitance requires a larger BK_{Ca} channel current and thus a larger total number of channels, if similar functions are to be performed. However, as long as we consider isopotential cells, these size factors cannot fully explain differences in channel densities by themselves, because both the channel number and membrane capacitance are proportional to the surface area. Nevertheless, the fact that each cerebellar PC is equipped with a massive dendritic tree, which dwarfs that of the DG granule cells, might be relevant. Thus, the dendrites, unless they have the same channel density as the soma, and the channels all activate almost simultaneously, may represent a large sink that may require a larger somatic channel density in cerebellar PC for achieving a similar impact compared to the less branched DG granule cells. In addition, there are likely to be several other, cell type-specific differences, including generation of dendritic Ca^{2+} spikes that can be regulated by BK_{Ca} channels (Rancz and Häusser, 2006).

Participation of BK_{Ca} channels in the formation of 'PLasmERosomes'

As in Purkinje cells, BK_{Ca} channels were clustered in the plasma membrane at sites of SSC in DG granule cells. Such cisterns are specialized subcompartments of the ER, which contributes crucially to spatial Ca^{2+} buffering and signaling in neurons (Verkhratsky, 2005). Increasing evidence suggests that neuronal ER does not represent a uniform Ca^{2+} pool but rather a spatially heterogeneous system encompassing multiple Ca^{2+} subdomains (calciosomes). These specialized ER domains are supposed to unload and refill Ca^{2+} independently (Blaustein and Golovina, 2001), and SSC are likely to represent such kind of calciosomes in central principal neurons. Areas of the plasma membrane overlying calciosomes also form specialized microdomains that contain unique sets of membrane proteins (Moore et al., 1993; Putney and Ribeiro, 2000). These domains are proposed to function as a coordinated unit, a "PLasmERosome", together with the underlying calciosome (Blaustein and Golovina, 2001). The present study demonstrating BK_{Ca} channel clustering in areas of the plasma membrane overlying SSC provides strong morphological evidence that BK_{Ca} channels participate in building such PLasmERosome in central principal neurons.

The presence of PLasmERosomes may be correlated with some of the distinctive physiological properties of the neuronal surface (Blaustein and Golovina, 2001). They seem to be important for regulating the membrane potential (Satin and Adams, 1987; Akita and Kuba, 2000), and may also play a role in shaping of action potentials and modulation of firing rate (Mikoshiba, 2007). They may even represent a signal initiation site through modulation of junctional ER Ca^{2+} content by altering the activity of local Na^{+} pump isoforms, local Ca^{2+} release events (Ca^{2+} sparks) or calcium induced Ca^{2+} release (CICR; Blaustein and Golovina, 2001).

Non-homogenous distribution of BK_{Ca} channels

Non-homogenous distribution of potassium channels in central neurons was reported previously for members of the voltage-gated potassium channel family, in particular $K_V2.1$ channels (Lim et al., 2000), $K_V4.2$ channels (Alonso and Widmer, 1997; Jinno et al., 2005), and $K_V4.3$ channels (Kollo et al., 2006, 2008). Although extrasynaptic channel clusters have been proposed to participate in novel forms of intercellular communication, the functional roles of such clusters are still far from being understood. Obviously, ion channel clustering induces local changes in the electrophysiological properties of the neuronal surface membrane. Although nerve cell membranes are often assumed to be uniform with respect to electrical properties like excitability, capacitance and resistance, there is mounting evidence for spatial compartmentalization and heterogeneity in signaling within neuronal subdomains (Berridge, 2006; Dai et al., 2009).

Regarding differential spatiotemporal Ca^{2+} activation, the scattered and the clustered pool of BK_{Ca} channels may play different roles in the processing and shaping of electrical signals. Whereas the scattered pool of channels may be involved primarily in rapid, transient events such as spike repolarization (Storm, 1987a; Shao et al., 1999; Gu et al., 2007), the clustered pool may convey slower and more long-lasting effects (slower activating and slower decaying) that are triggered by CICR. Depolarization-dependent Ca^{2+} influx through voltage-gated Ca^{2+} (Ca_V) channels may induce CICR from SSC during high-frequency activity, thus activating BK_{Ca} channels in the plasma membrane (Llano et al., 1994; Akita and Kuba, 2000). Clustered BK_{Ca} channels may also be activated via spontaneous CICR and hence may represent a spike-independent signal initiation site (Bardo et al., 2006). Anyway, CICR-triggered BK_{Ca} channel activation likely happens in a rather slow manner occurring only after repolarization of a spike unlike the more direct activation of BK_{Ca} channels upon Ca^{2+} influx through Ca_V channels (Storm, 1987b; Brenner et al., 2000; Fakler and Adelman, 2008). BK_{Ca} channels are thus opened already during or shortly after a spike in many neurons (Storm, 1987a,b; Lancaster and Nicoll, 1987; Hu and Storm, 2001b; Edgerton and Reinhart, 2003; Sausbier et al., 2004). With respect to the scattered BK_{Ca} channels, we observed no ER component

within less than 80 nm distance, which would be required for serving as an effective Ca^{2+} source. It seems most likely that scattered BK_{Ca} channels are activated within Ca_V-BK_{Ca} complexes. Within the six major groups of Ca_V channels known, L-type ($Ca_V1.2$), P/Q-type ($Ca_V2.1$) and N-type ($Ca_V2.2$) channels can all reliably activate BK_{Ca} channels within milliseconds if present at nanometer distances. A proteomic approach combining affinity purification with mass spectrometry showed that these Ca_V channel types indeed form macro-molecular complexes with BK_{Ca} channels (Fakler and Adelman, 2008). Hence, scattered BK_{Ca} channels could be activated during the brief depolarization phase of an action potential, thus providing a rapid K^+ conductance contributing to spike repolarization and a fAHP component (Storm, 1987a,b; Shao et al., 1999; Hu and Storm, 2001b; Sausbier et al., 2004; Gu et al., 2007).

The two pools of channels could also differ in their mediation of local and spatially directed chemical signals. Being part of macromolecular signaling complexes, BK_{Ca} channel activity can be modulated by a wide spectrum of physiologically relevant factors such as phosphorylation, oxidation, steroid hormones, and gases (NO, CO; Hou et al., 2009). Thus, the different pools of channels might be linked to different subcellular signaling pathways.

CONCLUSION

In conclusion, this study provides the first ultrastructural localization of BK_{Ca} channels in the somatic plasma membrane of various central principal neurons, and demonstrates a common organizational principle in the distribution of these channels. In all neuronal cell types we examined, BK_{Ca} channels form two, probably independent pools: one consisting of clustered and one of scattered channels in extrasynaptic membrane areas. These two pools differ most likely in their routes of Ca^{2+} activation, with clustered BK_{Ca} channels being in position for activation via Ca^{2+} release from internal stores, and scattered channels being activated via an ER independent mechanism. The pool of clustered BK_{Ca} channels may thus represent a key element of somatic PLasmERosomes with potent contributions to spatial signaling within central principal neurons.

Acknowledgments—This work was supported by a grant from the Innsbruck Medical University, MFI-4305 to W.A.K., the Austrian Science Fund (FWF) S102 to F.F., and by the Centre of Excellence Programme of the Norwegian Research Council (NFR/SFF) to J.F.S. The excellent technical assistance of Barbara Knoll-Kreidl and Dr. Barbara Kapelari at Innsbruck Medical University, Dept. Pharmacology (Austria), is gratefully acknowledged. We thank Dr. Michael Hess at Innsbruck Medical University, Div. Histology and Embryology, for support in high-pressure freezing, Prof. Hans-Günther Knaus at Innsbruck Medical University, Div. Molecular and Cellular Pharmacology, for providing BK_{Ca} channel antibodies and Prof. Peter Ruth at the University of Tuebingen, Inst. Pharmacy (Germany), for providing BK_{Ca} null mice. We also gratefully acknowledge Prof. Ryuichi Shigemoto and Dr. Yugo Fukazawa at the National Institute for Physiological Sciences, Div. Cerebral Structure (Japan), for continuous support and discussions concerning the SDS-digested freeze-fracture replica labeling technique.

REFERENCES

Adelman JP, Shen KZ, Kavanaugh MP, Warren RA, Wu YN, Lagrutta A, Bond CT, North RA (1992) Calcium-activated potassium channels expressed from cloned complementary DNAs. Neuron 9: 209–216.

Akita T, Kuba K (2000) Functional triads consisting of ryanodine receptors, Ca^{2+} channels, and Ca^{2+}-activated K^+ channels in bullfrog sympathetic neurons. Plastic modulation of action potential. J Gen Physiol 116:697–720.

Alonso G, Widmer H (1997) Clustering of KV4.2 potassium channels in postsynaptic membrane of rat supraoptic neurons: an ultrastructural study. Neuroscience 77:617–621.

Amaral DG, Witter MP (1995) Hippocampal formation. In: The rat nervous system, 2nd edn. (Paxinos G, ed), pp 443–493. San Diego, CA: Elsevier/Academic Press Inc.

Bardo S, Cavazzini MG, Emptage N (2006) The role of the endoplasmic reticulum Ca^{2+} store in the plasticity of central neurons. Trends Pharmacol Sci 27:78–84. Review.

Benhassine N, Berger T (2005) Homogeneous distribution of large-conductance calcium-dependent potassium channels on soma and apical dendrite of rat neocortical layer 5 pyramidal neurons. Eur J Neurosci 21:914–926.

Berridge MJ (2006) Calcium microdomains: organization and function. Cell Calcium 40:405–412.

Blaustein MP, Golovina VA (2001) Structural complexity and functional diversity of endoplasmic reticulum Ca^{2+} stores. Trends Neurosci 24:602–608. Review.

Brenner R, Chen QH, Vilaythong A, Toney GM, Noebels JL, Aldrich RW (2005) BK channel beta4 subunit reduces dentate gyrus excitability and protects against temporal lobe seizures. Nat Neurosci 8:1752–1759.

Brenner R, Jegla TJ, Wickenden A, Liu Y, Aldrich RW (2000) Cloning and functional characterization of novel large conductance calcium-activated potassium channel beta subunits, hKCNMB3 and hKCNMB4. J Biol Chem 275:6453–6461.

Cui J, Cox DH, Aldrich RW (1997) Intrinsic voltage dependence and Ca^{2+} regulation of mslo large conductance Ca^{2+}-activated K^+ channels. J Gen Physiol 109:647–673.

Dai S, Hall DD, Hell JW (2009) Supramolecular assemblies and localized regulation of voltage-gated ion channels. Physiol Rev 89:411–452. Review.

Edgerton JR, Reinhart PH (2003) Distinct contributions of small and large conductance Ca^{2+}-activated K^+ channels to rat Purkinje neuron function. J Physiol 548:53–69.

Faber ES, Sah P (2003) Calcium-activated potassium channels: multiple contributions to neuronal function. Neuroscientist 9:181–194. Review.

Faber ES, Sah P (2002) Physiological role of calcium-activated potassium currents in the rat lateral amygdala. J Neurosci 22:1618–1628.

Fakler B, Adelman JP (2008) Control of K(Ca) channels by calcium nano/microdomains. Neuron 59:873–881. Review.

Fujimoto K (1995) Freeze-fracture replica electron microscopy combined with SDS digestion for cytochemical labeling of integral membrane proteins. Application to the immunogold labeling of intercellular junctional complexes. J Cell Sci 108:3443–3449.

Geiger JR, Jonas P (2000) Dynamic control of presynaptic Ca(2+) inflow by fast-inactivating K(+) channels in hippocampal mossy fiber boutons. Neuron 28:927–939.

Golding NL, Jung HY, Mickus T, Spruston N (1999) Dendritic calcium spike initiation and repolarization are controlled by distinct potassium channel subtypes in CA1 pyramidal neurons. J Neurosci 19:8789–8798.

Grunnet M, Kaufmann WA (2004) Coassembly of big conductance Ca^{2+}-activated K^+ channels and L-type voltage-gated Ca^{2+} channels in rat brain. J Biol Chem 279:36445–36453.

Gu N, Vervaeke K, Storm JF (2007) BK potassium channels facilitate high-frequency firing and cause early spike frequency adaptation in rat CA1 hippocampal pyramidal cells. J Physiol 580:859–882.

Hou S, Heinemann SH, Hoshi T (2009) Modulation of BKCa channel gating by endogenous signaling molecules. Physiology 24:26–35. Review.

Hu H, Shao LR, Chavoshy S, Gu N, Trieb M, Behrens R, Laake P, Pongs O, Knaus HG, Ottersen OP, Storm JF (2001a) Presynaptic Ca^{2+}-activated K^+ channels in glutamatergic hippocampal terminals and their role in spike repolarization and regulation of transmitter release. J Neurosci 21:9585–9597.

Hu H, Storm JF (2001b) Differential BK channels contribute to action potential repolarization in granule cells of the rat dentate gyrus. Society for Neuroscience, program no 27:1002. Abstract.

Jinno S, Jeromin A, Kosaka T (2005) Postsynaptic and extrasynaptic localization of Kv4.2 channels in the mouse hippocampal region, with special reference to targeted clustering at gabaergic synapses. Neuroscience 134:483–494.

Kaufmann WA, Ferraguti F, Fukazawa Y, Kasugai Y, Shigemoto R, Laake P, Sexton JA, Ruth P, Wietzorrek G, Knaus HG, Storm JF, Ottersen OP (2009) Large-conductance calcium-activated potassium channels in purkinje cell plasma membranes are clustered at sites of hypolemmal microdomains. J Comp Neurol 515:215–230.

Knaus HG, Eberhart A, Koch RO, Munujos P, Schmalhofer WA, Warmke JW, Kaczorowski GJ, Garcia ML (1995) Characterization of tissue-expressed alpha subunits of the high conductance Ca^{2+}-activated K^+ channel. J Biol Chem 270:22434–22439.

Knaus HG, Schwarzer C, Koch RO, Eberhart A, Kaczorowski GJ, Glossmann H, Wunder F, Pongs O, Garcia ML, Sperk G (1996) Distribution of high-conductance Ca^{2+}-activated K^+ channels in rat brain: targeting to axons and nerve terminals. J Neurosci 16: 955–963.

Kolde G, Themann H (1982) Subsurface cisterns and lamellar bodies in the granule cells of the guinea-pig fascia dentata. Cell Tissue Res 223:455–461.

Kollo M, Holderith NB, Nusser Z (2006) Novel subcellular distribution pattern of A-type K^+ channels on neuronal surface. J Neurosci 26:2684–2691.

Kollo M, Holderith N, Antal M, Nusser Z (2008) Unique clustering of A-type potassium channels on different cell types of the main olfactory bulb. Eur J Neurosci 27:1686–1699.

Laatsch RH, Cowan WM (1966) Electron microscopic studies of the dentate gyrus of the rat. I. Normal structure with special reference to synaptic organization. J Comp Neurol 128:359–395.

Lancaster B, Nicoll RA (1987) Properties of two calcium-activated hyperpolarizations in rat hippocampal neurones. J Physiol 389: 187–203.

Latorre R, Brauchi S (2006) Large conductance Ca^{2+}-activated K^+ (BK) channel: activation by Ca^{2+} and voltage. Biol Res 39:385–401. Review.

Le Beux YJ (1972) Subsurface cisterns and lamellar bodies: particular forms of the endoplasmic reticulum in the neurons. Z Zellforsch Mikrosk Anat 133:327–352.

Lim ST, Antonucci DE, Scannevin RH, Trimmer JS (2000) A novel targeting signal for proximal clustering of the Kv2.1 K^+ channel in hippocampal neurons. Neuron 25:385–397.

Lingle CJ, Solaro CR, Prakriya M, Ding JP (1996) Calcium-activated potassium channels in adrenal chromaffin cells. Ion Channels 4: 261–301. Review.

Llano I, DiPolo R, Marty A (1994) Calcium-induced calcium release in cerebellar Purkinje cells. Neuron 12:663–673.

Masugi-Tokita M, Tarusawa E, Watanabe M, Molnár E, Fujimoto K, Shigemoto R (2007) Number and density of AMPA receptors in individual synapses in the rat cerebellum as revealed by SDS-digested freeze-fracture replica labeling. J Neurosci 27:2135–2144.

Matsubara A, Laake JH, Davanger S, Usami S, Ottersen OP (1996) Organization of AMPA receptor subunits at a glutamate synapse: a quantitative immunogold analysis of hair cell synapses in the rat organ of Corti. J Neurosci 16:4457–4467.

Meis S, Pape HC (1997) Properties of a Ca^{2+}-activated K^+ conductance in acutely isolated pyramidal-like neurons from the rat basolateral amygdaloid complex. J Neurophysiol 78:1256–1262.

Mikoshiba K (2007) IP3 receptor/Ca^{2+} channel: from discovery to new signaling concepts. J Neurochem 102:1426–1446. Review.

Misonou H, Menegola M, Buchwalder L, Park EW, Meredith A, Rhodes KJ, Aldrich RW, Trimmer JS (2006) Immunolocalization of the Ca^{2+}-activated K^+ channel Slo1 in axons and nerve terminals of mammalian brain and cultured neurons. J Comp Neurol 496: 289–302.

Moore ED, Etter EF, Philipson KD, Carrington WA, Fogarty KE, Lifshitz LM, Fay FS (1993) Coupling of the Na^+/Ca^{2+} exchanger, Na^+/K^+ pump and sarcoplasmic reticulum in smooth muscle. Nature 365:657–660.

Paxinos G (1995) The rat nervous system, 2nd edn. San Diego, CA: Elsevier/Academic Press Inc.

Paxinos G, Watson C (1998) The rat brain in stereotaxic coordinates, 4th edn. San Diego, CA: Elsevier/Academic Press Inc.

Putney JW Jr, Ribeiro CM (2000) Signaling pathways between the plasma membrane and endoplasmic reticulum calcium stores. Cell Mol Life Sci 57:1272–1286. Review.

Raffaelli G, Saviane C, Mohajerani MH, Pedarzani P, Cherubini E (2004) BK potassium channels control transmitter release at CA3-CA3 synapses in the rat hippocampus. J Physiol 557:147–157.

Rancz EA, Häusser M (2006) Dendritic calcium spikes are tunable triggers of cannabinoid release and short-term synaptic plasticity in cerebellar Purkinje neurons. J Neurosci 26:5428–5437.

Robitaille R, Garcia ML, Kaczorowski GJ, Charlton MP (1993) Functional colocalization of calcium and calcium-gated potassium channels in control of transmitter release. Neuron 11:645–655.

Sah P, Faber ES (2002) Channels underlying neuronal calcium-activated potassium currents. Prog Neurobiol 66:345–653. Review.

Sailer CA, Kaufmann WA, Kogler M, Chen L, Sausbier U, Ottersen OP, Ruth P, Shipston MJ, Knaus HG (2006) Immunolocalization of BK channels in hippocampal pyramidal neurons. Eur J Neurosci 24:442–454.

Salkoff L, Butler A, Ferreira G, Santi C, Wei A (2006) High-conductance potassium channels of the SLO family. Nat Rev Neurosci 7:921–931. Review.

Satin LS, Adams PR (1987) Spontaneous miniature outward currents in cultured bullfrog neurons. Brain Res 401:331–339.

Sausbier M, Hu H, Arntz C, Feil S, Kamm S, Adelsberger H, Sausbier U, Sailer CA, Feil R, Hofmann F, Korth M, Shipston MJ, Knaus HG, Wolfer DP, Pedroarena CM, Storm JF, Ruth P (2004) Cerebellar ataxia and Purkinje cell dysfunction caused by Ca^{2+}-activated K^+ channel deficiency. Proc Natl Acad Sci U S A 101:9474–9478.

Sausbier U, Sausbier M, Sailer CA, Arntz C, Knaus HG, Neuhuber W, Ruth P (2006) Ca^{2+}-activated K^+ channels of the BK-type in the mouse brain. Histochem Cell Biol 125:725–741.

Shao LR, Halvorsrud R, Borg-Graham L, Storm JF (1999) The role of BK-type Ca^{2+}-dependent K^+ channels in spike broadening during repetitive firing in rat hippocampal pyramidal cells. J Physiol 521:135–146.

Storm JF (1987a) Action potential repolarization and a fast after-hyperpolarization in rat hippocampal pyramidal cells. J Physiol 385:733–759. Review.

Storm JF (1987b) Intracellular injection of a Ca^{2+} chelator inhibits spike repolarization in hippocampal neurons. Brain Res 435:387–392.

Storm JF (1990) Potassium currents in hippocampal pyramidal cells. Prog Brain Res 83:161–187. Review.

Takumi Y, Ramírez-León V, Laake P, Rinvik E, Ottersen OP (1999) Different modes of expression of AMPA and NMDA receptors in hippocampal synapses. Nat Neurosci 2:618–624.

Triller A, Choquet D (2005) Surface trafficking of receptors between synaptic and extrasynaptic membranes: and yet they do move! Trends Neurosci 28:133–139. Review.

van Lookeren Campagne M, Oestreicher AB, van der Krift TP, Gispen WH, Verkleij AJ (1991) Freeze-substitution and Lowicryl HM20 embedding of fixed rat brain: suitability for immunogold ultrastructural localization of neural antigens. J Histochem Cytochem 39:1267–1279.

Verkhratsky A (2005) Physiology and pathophysiology of the calcium store in the endoplasmic reticulum of neurons. Physiol Rev 85: 201–279. Review.

Wanner SG, Koch RO, Koschak A, Trieb M, Garcia ML, Kaczorowski GJ, Knaus HG (1999) High-conductance calcium-activated potassium channels in rat brain: pharmacology, distribution, and subunit composition. Biochemistry 38:5392–5400.

Wei AD, Gutman GA, Aldrich R, Chandy KG, Grissmer S, Wulff H (2005) International Union of Pharmacology. LII. Nomenclature and molecular relationships of calcium-activated potassium channels. Pharmacol Rev 57:463–472. Review.

Womack MD, Khodakhah K (2002) Characterization of large conductance Ca^{2+}-activated K^{+} channels in cerebellar Purkinje neurons. Eur J Neurosci 16:1214–1222.

(Accepted 27 May 2010)
(Available online 4 June 2010)